European Food Research and Technology
https://doi.org/10.1007/s00217-024-04538-4

ORIGINAL PAPER

Comparative study of thermal behavior of mango kernel fat from seven Ivorian varieties related to their chemical composition

Alfred Kouakou Kouassi[1] · Taofic Alabi[2,6] · Elise Amoin N'guessan[5] · Giorgia Purcaro[3] · Sabrina Moret[4] · Mohamed Cissé[5] · Christophe Blecker[1] · Sabine Danthine[1]

Received: 12 January 2024 / Revised: 15 March 2024 / Accepted: 16 March 2024

Abstract

In the present study, the fatty acid composition (FAC), triacylglycerol (TAG) composition, crystallization, and melting behaviors of mango kernel fats (MKFs) extracted from seven Ivorian mango varieties—*Amelie* (AM), *Kent* (KT), *Palmer* (PR), *Keitt* (KI), *Brooks* (BR), *Dadiani* (DI), and *Djakoumankoun* (DN)—were characterized by complementary techniques: pNMR, DSC, polarized light microscopy, and X-ray diffraction. Regardless of the variety, Ivorian MKF is rich in stearic (St) and oleic (O) fatty acids. (72–84% of the total FA), with three main TAGs: StOSt (23.9–45.8%), StOO (15.5–25.8%), and StLSt (10.4–12.5%). Their crystallization onset temperature (Tco) ranged from 15 to 20 °C. All samples showed complete melting around 35 °C, except DN (~ 38 °C). The β-polymorph appeared to be the most predominant and stable polymorph for the seven MKFs. The thermal properties investigated were linked to monounsaturated and triunsaturated triacylglycerol content, indicating the significant influence of chemical composition. The fine analysis of the results allows the seven Ivorian varieties to be divided into four groups, based on both their physical properties and thermal behavior, and the StOSt wealth: hard high-StOSt fat (DN), half-hard medium-StOSt fat (DI, BR), soft low-StOSt fat (KT, PR, KI), and very-soft very-low-StOSt fat (AM). The seven investigated mango varieties from Ivory Coast might offer a wide range of applications in food, pharmaceutical, and cosmetic industries.

Keywords Mango kernel fat · Ivorian varieties · Fatty acid composition · Triacylglycerol · Crystallization · Melting behavior · Polymorphism · Solid fat content

Introduction

Vegetable fats and oils, usually derived from oilseeds, nuts, or fruits, are widely used in the food, pharmaceutical, cosmetic, and chemical industries. Driven by the increasing consumption of high-quality edible oils and fats for everyday food and the growing demand for non-food sector, the need for new vegetable fat sources continues unabated. Agro-industrial residues may become important unconventional sources for some applications.

Mango (*Mangifera indica* L) is the most popular fruit in Ivory Coast. The average production of fresh mango is over 150,000 tons per year [1]. Large quantities of seed, the major by-product from mango processing and consumption remain unused. According to Lakshminarayana et al. [2] and Nzikou et al. [3], mango seed kernels contain an interesting amount of fat: 3.7 to 15% (on dry basis), making them a valuable source for edible fat recovery. This hidden resource of mango kernel can generally be extracted by cold pressing

✉ Alfred Kouakou Kouassi
akouassi@uliege.be

1 Food Science and Formulation, University of Liège-Gembloux Agro-Bio Tech, Gembloux, Belgium

2 Department of Animal Biology, University Peleforo Gon Coulybaly, Korhogo, Ivory Coast

3 Analytical Chemistry, University of Liège-Gembloux Agro-Bio Tech, Gembloux, Belgium

4 Environment and Animal Sciences, Agri-Food, University of Udine, Udine, Italy

5 Department of Biochemistry and Genetic, University Peleforo Gon Coulybaly, Korhogo, Ivory Coast

6 Functional and Evolutionary Entomology, University of Liège-Gembloux Agro-Bio Tech, Gembloux, Belgium

Published online: 11 April 2024

and solvent extraction. Mango kernel fat (MKF) has compositional and physicochemical characteristics that make it a potential alternative to processed semisolid edible fats high in trans fatty acids, which have serious negative effect on human health [4]. In addition, MKF is one the six vegetable fats allowed to be used as a cocoa butter equivalent (CBE) by the European Union (Directive 2000/36/EC) [5]. CBE are vegetables fats which exhibit physicochemical properties similar to those of cocoa butter (CB); they have been used in confectionary products for several years. Considering this, Ivory Coast mango might be an interesting source of edible fat.

Since physical and thermal properties of fats and oils are essential to understand their functionality in fat-based products, the properties of MKF have attracted attention due their valuable role in CB formulations and confectionary. Kaur et al. [6] recently analyzed and characterized MKF as cocoa butter substitute and indicated that it can be used in place of cocoa butter.

However, a variety-dependent chemical composition (fatty acids, triacylglycerols) and thermal behavior of MKF have been reported in previous studies [7–9]. Recently, we extracted and chemically characterized MKFs from seven specific Ivory Coast varieties and found that they were significantly different in chemical composition from each other [10]. The differences observed in FAC and TAG between the seven varieties suggest that their physical properties and thermal behavior would differ. In a very recent publication of the authors [11], the polymorphic behavior during isothermal crystallization of MKF from three selected varieties was investigated. However, no information has been published on the physicochemical and thermal properties of the MKF of the seven varieties, which were only chemically characterized in their first study [10]. In light of this, the study reported here aims at filling this gap, as it investigates the crystallization and melting behavior of MKF from these seven Ivorian varieties using differential scanning calorimetry (DSC), pulsed nuclear magnetic resonance (pNMR), powder X-ray diffraction (XRD), and polarized light microscope (PLM).

Thus, the purpose of work is to improve knowledge of the physicochemical and thermal characteristics displayed by Ivorian MKFs, as these are fundamental characteristics for developing new products based on fats.

Material and methods

Samples

Mango seeds of five grafted varieties; *Kent* (KT), *Amelie* (AM), *Brooks* (BR), *Palmer* (PR), *Keitt* (KI) cultivated in Korhogo province (Ivory Coast), were supplied by local dried mango processing companies. Two local mango varieties, *Dadiani* (DI) and *Djakoumankoun (DN),* were also collected in the same province and were separated from pulps. All mango seeds were sun-dried for 2 days and then shelled to remove the kernels, which were sun-dried to constant weight for about 2 weeks. The samples were subsequently ground to a 1 mm particle size using a high-speed lab grinder (FRITSCH, 19.1020/00426, ROHS, Oberstein, Germany). The obtained powders were stored at 4 °C until use in closed plastic containers under vacuum.

The fat was extracted from the so obtained powder using maceration at 40 °C with stirring for 90 min, using *n*-hexane as solvent as described by Kouassi et al. [10]. The extracted fats were further stored in the dark at − 20 °C until analyses.

Fatty acid composition (FAC) by gas chromatography (GC)

FAC was determined as described by Mtibaa et al. [12] using a Trace GC Ultra gas chromatograph (GC) (Thermo Fisher Scientific, Belgium) equipped with a flame ionization detector (FID). The analysis was carried out in triplicate and the results are expressed as the mean ± standard deviation.

Triacylglycerol composition

Triacylglycerol (TAG) composition was determined as described in our recent paper [10], using an HPLC Infinity II 1260 system (Agilent Technologies Inc., Santa Clara, CA, USA) equipped with a refractive index detector (RID) and a C18 column (RP-18 LiChroCART 250-4 5 µm, 250 mm × 4 mm, Merck, Darmstadt, Germany). Data are presented as the average of two replicates for each sample.

Melting profiles by pNMR

The melting behavior of each extracted MKF was analyzed by means of pNMR between 5 °C and 40 °C, using a Minispec-mq20 spectrometer (Bruker, Karlsruhe, Germany) according to the IUPAC method 2.150 (ex 2.323) [13]. Two methods were used: an untempered serial method for routine use and a serial method with fat conditioning (40 h at 26 °C). Data are presented as the mean of three independent measurements.

Crystallization and melting profiles by differential scanning calorimetry (DSC)

DSC melting profiles were determined using aluminum T0 hermetic pans according to the method described by Danthine [14] using a Q2000 DSC equipped with a refrigerated cooling system (TA Instruments, New Castle, USA). Calibration was carried out using indium (melting point:

156.6 °C) and *n*-dodecane (melting point: − 9.56 °C). Nitrogen was used as the purge gas to avoid the formation of condensation in the cells. The samples (2–4 mg) were placed in the pans, and an empty similar pan was used as a reference. The AOCS method (Cj 1-94) [15] was used to set the time–temperature program: samples were first heated to 80 °C to ensure complete melting and held at this temperature for 10 min. They were then cooled to − 60 °C with a cooling rate of − 10 °C/min and held at − 60 °C for 30 min before further heating at a rate of 5 °C/min to record the melting profiles from − 60 °C to 80 °C. DSC analyses were conducted in duplicate. Universal Analysis Software version 4.2 (TA Instruments, New Castle, USA) was used for peak temperature and enthalpy measurements. All the measurements were performed in triplicate.

Crystal morphological

Polarized light microscopy (PLM) using a Nikon microscope (Nikon Optical Co., Ltd., Tokyo, Japan) equipped with a digital camera (Sight DS-U3, Nikon Optical Co., Ltd., Tokyo, Japan) was used to observe the crystal network microstructure of the fats crystallized at 20 °C under static conditions. After complete melting of the fat at 80 °C for 10 min to eliminate crystal memory, 20 µL of each sample was placed on a glass microscope slide, pre-heated to 80 °C before use. A pre-heated glass coverslip was carefully placed on top of the sample to create a film of uniform thickness. The samples were then incubated for 24 h at 20 °C in a temperature-controlled chamber. A tenfold objective lens was used. Three replications were performed.

Polymorphism

The polymorphic behavior of the MKFs was investigated by powder X-ray diffraction (XRD) using a Bruker D8 Advance diffractometer (Bruker, Karlsruhe, Germany) (ƛ Cu = 1.54178 Å, 40 kV, 30 mA) equipped with an Anton Paar (Graz, Austria) temperature control system consisting of a TTK 450 low temperature chamber and a TCU 110 heater, and a Lynxeye detector (Bruker, Karlsruhe, Germany). Short-spacing (15–27° 2θ) and long-spacing (1–13° 2θ) runs were recorded. Diffrac EVA V3.0 software (Bruker, Karlsruhe, Germany) was used to analyze the diffraction patterns and determine the d-values according to the Bragg law. The fat sample was completely melted for 10 min at 80 °C to eliminate the memory effect and then the samples were rapidly placed for 24 h in a temperature-controlled cabinet set at 20 ± 0.5 °C. After this period, the samples were placed in an XRD sample holder and analyzed at 20 °C. The sample holder was brought to 20 °C before use. All the analysis were conducted in triplicate.

Statistical analysis

Minitab 21 software (Minitab Inc., Coventry, UK) was used for ANOVA one-way and Tukey's test ($p < 5\%$, significant difference).

Results and discussion

Chemical characterization of MKFs

Fatty acid composition

FAC of the seven extracted MKFs, shown in Table 1, was already deeply and extensively discussed in comparison with the literature [10]. Only a comparative analysis between the samples is made here to help understand FAC involvement in physical and thermal properties discussed in the following section "Melting and crystallization properties". Oleic acid (O—C18:1) and stearic acid (St—C18:0) are the major fatty acids in the seven samples, ranging from 35.9 to 47.9% and from 30.3 to 48.3%, respectively; they are followed by palmitic acid (P, C16:0), from 8.3 to 13.4%. In addition to these FAs, linoleic (L, C18:2) (up to 10%), linolenic (Ln, C18:3), and arachidic (A, C20:0) acids are minor FAs present in MKFs. The predominance of C18:1, C18:0, and C16:0 ranged from 87.6 to 93.5% of the total fatty acids. This high predominance shows MKF resembles other natural fats like cocoa butter (*Theobroma cacao*), illipe butter (*Shorea stenoptera*), sal (*Shorea robusta*), and shea butter (*Butyrospermum parkii*), which are specifically permitted to produce CBE and widely used in food processing. In cocoa butter, these three fatty acids represent approximately 95% of total FAC [7]. The FAC of the seven samples varied considerably depending on the varieties. Among them, DN contained a significantly higher amount of C18:0 (48.3%), while samples AM had the lowest (30.3%). For C18:1, PR had the highest content and DN the lowest one. For C16, AM contained a significantly higher content (13.4%) and DN had the lowest. In addition, AM had a significantly higher content of the C18:2 and C18:3, while DN had the lowest contents of these two essential FAs. For arachidic acid, DN had the highest content and AM contained the lowest one. Different trends were found for the two major FA, stearic and oleic acids. DN contained higher content of stearic acid than oleic acid, while for BR and DI, these two FA had comparable contents. Contrarily, oleic acid predominated in AM, KI, KT, and PR, followed by stearic acid. The total SAFA content ranged from 45 to 59%, with DN having the highest content and AM the lowest, while the un-SAFA ranged from 41 to 55%, with PR showing the highest and DN the lowest content. Moreover, AM stands out for its significantly higher proportion of PUFA (10.7%) compared to the other samples

Table 1 Fatty acid composition (%total fat means ± SD) and triacylglycerol composition (as average of two replicates) of various Ivorian MKFs

FA	Fatty acid composition						
	AM	BR	DI	DN	KI	KT	PR
C16:0	13.4 ± 0.9^{a}	8.7 ± 0.4^{c}	9.5 ± 0.2^{bc}	8.3 ± 0.12^{c}	10.6 ± 0.03^{b}	9.4 ± 0.04^{bc}	9.4 ± 0.16^{bc}
C18:0	30.3 ± 2.27^{d}	42.5 ± 0.57^{b}	40.6 ± 0.08^{b}	48.3 ± 0.02^{a}	35.6 ± 1.02^{c}	35.1 ± 0.01^{c}	34.3 ± 1.79^{cd}
C20:0	1.7 ± 0.23^{c}	2.2 ± 0.21^{bc}	1.7 ± 0.05^{c}	2.3 ± 0.02^{b}	1.7 ± 0.13^{c}	1.8 ± 0.08^{bc}	1.7 ± 0.15^{c}
SFA	45.4 ± 1.61^{e}	53.4 ± 0.76^{bc}	52 ± 0.06^{cd}	59 ± 0.09^{a}	48 ± 0.92^{de}	46.3 ± 0.13^{e}	45.4 ± 1.09^{e}
C18:1n9	44 ± 0.66^{bc}	41.2 ± 0.66^{cd}	41.4 ± 0.01^{cd}	36 ± 0.09^{e}	45.5 ± 0.52^{ab}	47 ± 0.03^{a}	48 ± 1.62^{a}
C18:2n6	9.6 ± 1.91^{a}	5.2 ± 0.06^{bc}	6.4 ± 0.02^{bc}	4.9 ± 0.02^{b}	6.1 ± 0.12^{b}	6.2 ± 0.23^{b}	6.3 ± 0.37^{b}
C18:3n3	1.1 ± 0.36^{a}	0.2 ± 0.05^{b}	0.3 ± 0.02^{b}	0.3 ± 0.02^{b}	0.4 ± 0.02^{b}	0.5 ± 0.07^{b}	0.5 ± 0.11^{b}
PUFA	10.7 ± 2.27^{a}	5.4 ± 0.10^{e}	6.7 ± 0.04^{c}	5.2 ± 0.01^{f}	6.5 ± 0.10^{d}	6.7 ± 0.09^{c}	6.8 ± 0.47^{b}
UFA	54.6 ± 1.67^{a}	46.6 ± 0.76^{cd}	48.1 ± 0.06^{bc}	41.1 ± 0.09^{e}	52 ± 0.92^{ab}	53.7 ± 0.13^{a}	54.7 ± 2.09^{a}
TAG	Triacylglycerol composition						
LLL	0.3	0.1	0.1	tr	0.1	0.2	0.1
OLLn	0.2	0.1	tr	tr	tr	0.1	0.1
OLL	1.9	0.9	1	0.6	1.1	1.3	0.9
OOL	3.1	1.6	1.8	0.9	2.1	2.3	2.2
OOO	7.8	4.8	4.8	2.5	7.3	8.4	7.9
PLLn	0.3	0.1	0.1	0.1	0.1	0.1	0.11
PLL	0.4	0.1	0.1	0.1	0.1	0.2	0.8
POLn	0.5	0.3	0.3	0.2	0.5	0.4	0.3
StLO + OOP	11	7.5	8.7	5.2	9.3	10.1	8.9
StLL + POL	3.5	1.8	2	1.3	2.1	2.3	1.9
AOO	2.5	2	1.7	1.5	2.2	2.2	2,3
StOO	20.8	20.7	23	15.5	22.6	25.8	25.5
PLP	1	0.3	0.4	0.4	0.4	0.5	0.3
PLnP	0.1	tr	tr	tr	tr	tr	tr
StLP	2.7	1.9	2	2.16	2	2	1.9
POP	2.6	1.3	1.5	1.2	1.7	1.5	1.3
StOP	3.9	4.6	4.6	6	3.4	3.5	3.3
StLSt	11.5	11.7	12.5	12	12.2	10.5	11.4
StOSt	24	37	33	45.8	29.4	26.3	29.7
AOSt	2.6	3.5	2.6	4.3	3.4	2.2	2.8
Monounsaturated TAGs (SUS)	53.2	64	61	74.6	57.2	51.6	54.1
Diunsaturated TAGs (SUU)	33.5	28.7	31.5	21.4	32.3	36.1	34.7
Triunsaturated TAGs (UUU)	13.3	7.4	7.6	4	10.5	12.4	11.2
Trisaturated TAGs (SSS)	0	0	0	0	0	0	0

St stearic, *O* oleic, *P* palmitic, *L* linoleic, *Ln* linolenic, *A* arachidic, *S* saturated, *U* unsaturated, *tr* trace; ≤ 0.05, *SFA* saturated fatty acids, *PUFA* polyunsaturated fatty acids, *UFA* unsaturated fatty acids (sum of mono- and polyunsaturated fatty acids), *KI* Keitt, *AM* Amelie, *BR* Brooks, *KT* Kent, *PR* Palmer, *DI* Dadiani, *DN* Djakoumankoun

Significant differences of means ($p \leq 0.05$) within a row are indicated by different letters

examined here, ranging from 5.2 to 6.8% only. The changes in the FAC of the MKFs studied will result in a large variability of triacylglycerols.

Triacylglycerol (TAG) composition

The consideration regarding the discussion for the FAC is applicable here as well. As expected, StOSt (24–46%) is the predominant TAG in the seven samples [10, 16]. Triacylglycerol compositions of the seven fats are given in Table 2, where it can be seen that MKFs contained: mono-unsaturated TAGs (SUS, 51–75%), di-unsaturated TAGs (SUU, 21–36%) and triunsaturated TAGs (UUU, 3–14%). No trisaturated TAG (SSS) were identified in any of the seven MKFs. The main TAGs found in the seven samples were StOSt (24–46%), StOO (15–26%), and StLSt (10–13%). The MKFs

Table 2 Crystallization and melting characteristics of different Ivorian MKFs

Mango variety	ΔH (J/g)	T_{co} (°C)	Temperature of transition point (°C)					T_{mc} (°C)
			*T*1	*T*2	*T*3	*T*4	*T*5	
Crystallization								
KI	62.66 ± 0.02	17.01 ± 0.01	16.36 ± 0.01	9.31 ± 0.01	− 1.72 ± 0.01			
AM	57.06 ± 0.08	14.72 ± 0.01	13.97 ± 0.01	8.76 ± 0.01	− 1.81 ± 0.01			
BR	66.68 ± 0.02	18.03 ± 0.04	17.38 ± 0.01	9.81 ± 0.01	− 1.50 ± 0.01			
KT	62.76 ± 0.01	15.39 ± 0.02	14.81 ± 0.01	9.02 ± 0.01	− 1.71 ± 0.02			
PR	63.88 ± 0.02	16.44 ± 0.01	15.77 ± 0.01	9.37 ± 0.02	− 1.73 ± 0.01			
DI	66.01 ± 0.01	17.12 ± 0.02	16.19 ± 0.02	8.94 ± 0.01	− 1.61 ± 0.01			
DN	71.22 ± 0.02	19.63 ± 0.01	18.97 ± 0.01	9.95 ± 0.01	− 1.48 ± 0.01			
Melting								
KI	66.06 ± 0.08		− 3.09 ± 0.01	11.67 ± 0.01	13.40 ± 0.02	16.73 ± 0.01	23.74 ± 0.01	35.05 ± 0.07
AM	59.97 ± 0.02		− 3.12 ± 0.02	8.09 ± 0.01	9.81 ± 0.03	13.32 ± 0.01	21.76 ± 0.03	34.68 ± 0.01
BR	68.57 ± 0.01		− 2.54 ± 0.02	9.15 ± 0.02	16.71 ± 0.01	26.80 ± 0.02		35.09 ± 0.01
KT	65.03 ± 0.04		− 3.06 ± 0.01	9.55 ± 0.01	11.35 ± 0.03	14.88 ± 0.02	24.14 ± 0.01	34.89 ± 0.04
PR	65.26 ± 0.02		− 3.04 ± 0.04	10.39 ± 0.01	12.60 ± 0.02	15.75 ± 0.01	24.41 ± 0.02	34.88 ± 0.01
DI	69.29 ± 0.03		− 3.34 ± 0.01	11.01 ± 0.02	13.13 ± 0.01	15.69 ± 0.02	26.27 ± 0.01	35.06 ± 0.03
DN	73.75 ± 0.01		− 2.95 ± 0.01	11.94 ± 0.01	18.97 ± 0.02	28.12 ± 0.01	30.78 ± 0.02	38 ± 0.02

KI: Keitt; AM: Amelie; BR: Brooks; KT: Kent; PR: Palmer; DI: Dadiani; DN: Djakoumankoun

ΔH, enthalpy; T_{co}: crystallization onset temperature; T_{mc}: melting completion temperature

also contained significant content of OOO (2–9%) and StOP (3–5%). Among MKFs of the seven varieties, DN had the higher SUS content (74,7%, mainly StOSt, StLSt), followed by BR and DI (64 and 61%, respectively), while AM, PR, and KT contained the lower one. Contrarily, the latter had significantly higher contents of SUU and UUU TAGs, while DN, BR, and DI contained lower contents. Note that sample DN stands out with its high StOSt content (45.8%) and low UUU content (4%). Conversely, AM is characterized by its high UUU content (13.3%) and lower StOSt content compared to the other samples. This result undoubtedly shows that the TAG composition depends on the mango variety. Based on the differences and similarities in TAG composition, Kouassi et al. [10] recently classified the seven varieties under study into four groups: group I = AM, group II = KI, PR, KT, group III = BR, DI and, group IV = DN.

Melting and crystallization properties

Crystallization and melting profiles by differential scanning calorimetry (DSC)

The crystallization and melting thermograms obtained by the DSC for the seven MKF are reported in Fig. 1. The crystallization onset temperature (T_{co}), melting completion temperature (T_{mc}), the enthalpy (ΔH) of crystallization and of melting, and the temperature of exothermic and endothermic transition peaks are reported in Table 2. The crystallization curves of all MKF (Fig. 1a) showed mainly three distinct exothermic transitions (major exothermic regions), which may correspond to three main TAG groups (SUS, SUU, and UUU, respectively). Fat crystallization started at 15–20 °C and ended between − 10 and − 13 °C with a maximum peak at 21–14 °C. Among the seven varieties, DN had the highest T_{co} value (19.6 °C), while AM had the lower (14.7 °C). The different crystallization behaviors of the MKFs studied is due to the degree of saturation in fats. The increase of crystallization temperature is related to a higher proportion of monounsaturated TAGs (SUS, mainly StOSt) and likely in association with TAGs with long-chain fatty acids (e.g., C20). T_{co} is correlated to StOSt TAGs in combination with AOSt TAGs. Thus, the outstanding high T_{co} (19.6 °C) of DN can be attributed to the latter. In contrast, the higher degree of triunsaturated TAGs results in the delayed crystallization of AM (13.3% UUU). However, it should be noted that regardless of the chemical composition of the fats, the thermal curve is scanning rate dependent, making it difficult to compare results from other studies using different scanning rates or calorimeters. Thus, crystallization onset temperatures of the varieties studied were compared with those reported in MKFs for the same varieties, using the same rate of cooling (− 10 °C/min). Keitt and Palmer varieties showed higher values of T_{co} than those indicated by Lieb et al. [17] for the same varieties cultivated in Costa Rica (13.9 °C) and Brazil (11.7 °C), respectively. These differences are related to variations in their triacylglycerol composition. The crystallization enthalpies were low for AM (57.1 J/g)

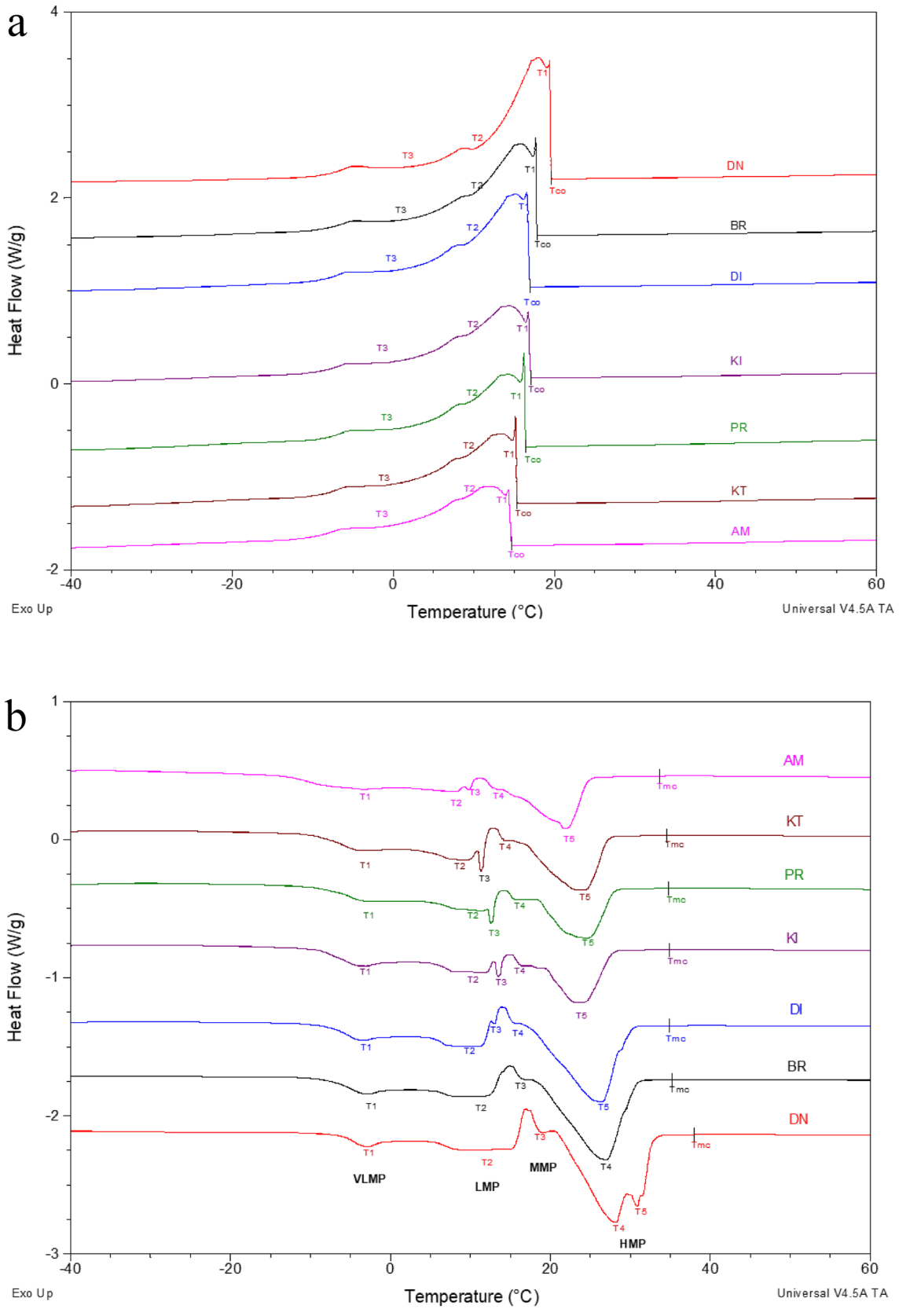

Fig. 1 DSC crystallization thermograms (**a**) and melting thermograms (**b**) of MKFs. KI: Keitt; AM: Amelie; BR: Brooks; KT: Kent; PR: Palmer; DI: Dadiani; DN: Djakoumankoun

and high for DN (71.2 J/g), compared to the five other samples (62.7–68.2 J/g).

The DSC melting curves of the seven varieties of MKF are presented in Fig. 1b. All the melting curves were different and complex. The diversity of the TAG composition of MKF is responsible for this complexity. However, very close similarities were found on the melting profiles of KT and PR. This is linked to the similarity in the TAGs composition of these fats. As illustrated in the Fig. 1b, several endothermic transitions were detected corresponding to melting peaks of different TAG groups with different composition of fatty acids. Moreover, four mains distinct melting point regions were clearly apparent in general: the very-low-melting point (VLMP), low-melting point (LMP), medium-melting point (MMP), and high-melting point (HMP) with shoulders, which are related to the three major TAG groups (UUU, SUU, and SUS). All the MKF studied melted completely around 35 °C, except for DN which showed a complete melting at 38 °C. Simple melting profile of MKF from Manila variety (Mexico) was reported by Solís-Fuentes and Duran-de-Bazua [7]. Their study showed two melting point fractions, with complete fat melting observed around 58.8 °C. Jahurul et al. [18] found a similar melting curve of MKF to that of Solís-Fuentes and Duran-de-Bazua [7]. Unfortunately, neither the variety of mango nor its the origin was mentioned. In contrast, Lieb et al. [17] reported complex melting profiles for MKF from Costa Rica, Brazil, and Thailand, with a complete melting point between 27 and 36 °C. These different results are caused by the different degrees of unsaturation and to the conditions of the DSC scanning. When the melting profiles of some varieties studied were compared to those reported in MKF for the same varieties and using the same DSC scanning conditions, Keitt and Palmer varieties showed higher T_{mc} than values reported by Lieb et al. [17] (27.4 and 39.5 °C, respectively) for the same varieties grown in Costa Rica and Brazil, respectively. This difference is undoubtedly related to the variation in TAG composition.

In our study, the VLMP region is correlated to UUU content, the LMP region is most probably due to SUU, the MMP to the relative contributions of SUU and SUS, while the HMP region is entirely due to the SUS content. It was noticed that, for DN sample, one endo sub-peak was observed in the right part of the HMP, in the range of 29–40 °C, being linked to SUS with long fatty acid chains. Therefore, the high T_{mc} of DN was attributed to its highest content of SUS TAGs and more precisely linked to the StOSt, which is the main SUS TAG and AOSt high content, which were more abundant in DN fat than the other varieties, while the lowest T_{mc} of AM is attributed to its high proportion of UUU TAGs. The total melting enthalpy (ΔH) ranged between 59 and 74 J/g. The highest total melting enthalpy (Δ*H* 73.8 J/g) is observed for DN with the highest HMP contribution, while AM gave the lowest total melting enthalpy (Δ*H* 59.97 J/g) in correlation with the lowest HMP and highest VLMP and LMP contributions.

SFC melting profile by pNMR

Solid fat content (SFC) is an important parameter that can be used as a guide to assess whether a particular oil, fat or blend is suitable for a specific application [19]. Figures 2 and 3 show SFC melting profile of all MKFs measured at different temperatures between 5 and 40 °C. Among the seven samples investigated, the SFC of DN was the highest, followed by BR, DI, KT, KI, PR, and AM. This behavior is linked to differences in the fat composition. MKF with high content of SAFAs and with high proportions of monounsaturated TAGs (SUS, mainly StOSt) and low content of triunsaturated TAGs (UUU) had the highest SFC values. DN had the highest content of SAFA and highest content of SUS TAG while AM had lower SUS TAGs and the highest UUU TAGs. Without any tempering as showed in Fig. 2, within the range of 0 to 15 °C, all samples had over 40% of SFC. Between 15 and 30 °C, the SFC of all MKFs considerably decreased. The largest decrease in SFC values was detected between 15–20 °C for KT, PR, KI, and AM, while it ranged between 20–25 °C for DI and BR, and between 25–30 °C for DN. The SFC determined below room temperature (25 °C) characterizes the hardness of fat, while the value determined at a temperature between 25 and 30 °C indicates the heat resistance. A high SFC at temperature above 37 °C (body temperature) causes a waxy mouthfeel [20]. DN had the highest hardness, while AM had the lower one. The hardness was similar for BR and DI, and for KT and PR. Therefore, the different MKFs can be grouped into four distinct subgroups: Hard fat (only DN, 84.2% of SFC), medium-hard fat (DI, BR, 77–78% of SFC, respectively), soft fat (KT, PR, KI, 67–69% of SFC, respectively), and very-soft fat (AM, 53.8% SFC). This distinction is the same as the one established by Kouassi et al. [10] for the TAG composition, which

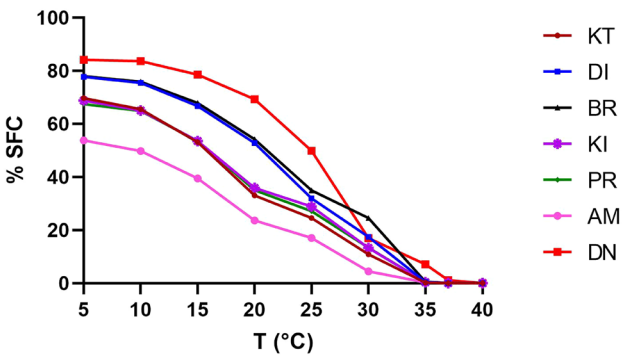

Fig. 2 Melting profile of MKFs obtained by pNMR without any tempering

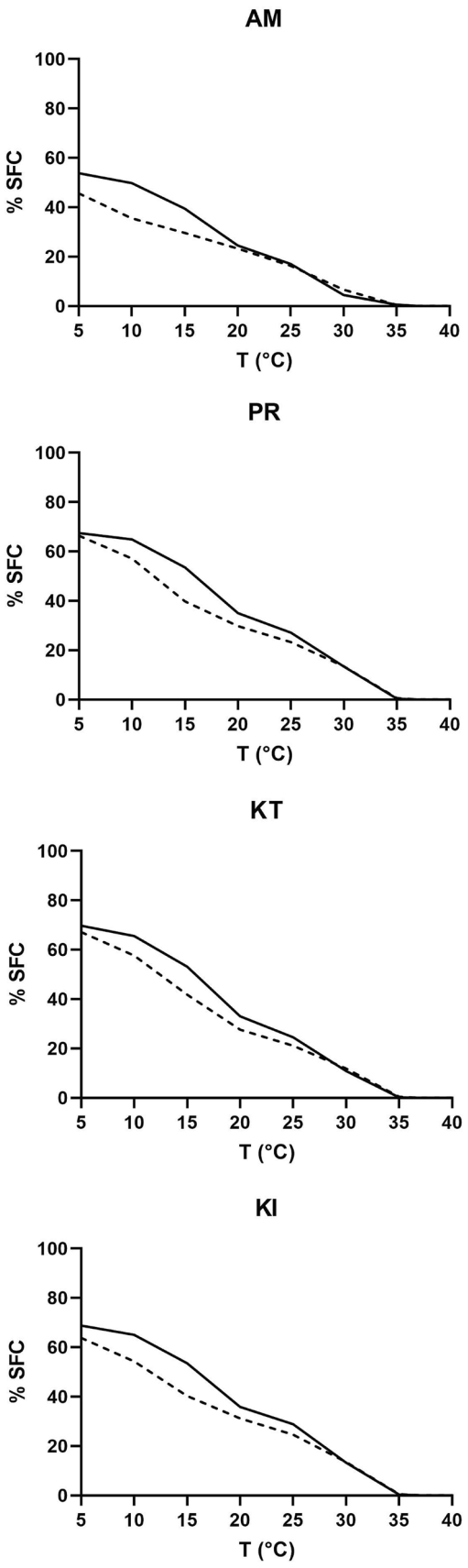

Fig. 3 pNMR melting profiles of MKFs, without any tempering (solid line) and after tempering at 26 °C for 40 h (dashed line)

clearly shows that TAG composition affects significantly the physical properties of the MKF. These differences might offer a wide range of applications in the food, pharmaceutical, and cosmetic industries. Moreover, except for DN, all MKFs were completely melted around 35 °C, where that of DN still showed SFC of 7.1%. Complete melting of DN occurs at 38 °C, 3 °C higher than the others, which does not lead to a waxy mouthfeel. The higher amount of SUS TAGs, more specifically StOSt, combined with AOSt, gives rise to a higher SFC at higher temperatures ($T > 30$–35 °C), where most of the other TAGs are liquid. On the other hand, due to its low SUS and high UUU content, AM had the lowest melting point. Furthermore, similarities in the thermal behavior of KT and PR are also clear in Fig. 2. This is linked to the similarity of their TAGs composition. These results are consistent with what was observed from DSC analysis (see section "Melting and crystallization properties").

In Fig. 3, a comparison of the results of untempered and tempered procedures is shown. When a fat is untempered or under tempered, different polymorphic forms exist, resulting in a broader melting range. On the other hand, during a tempering process, the crystals are converted to the more stable polymorph, giving rise to a very narrow melting range [21, 22]. In this study, the tempering at 26 °C affected the SFC melting profile of each MKF differently. The SFC at different temperatures differed widely as well as the total shape of SFC curves. According to Timms [21], below the tempering temperature, the SFC of a tempered sample is lower than that of an untempered fat. Above the tempering temperature, the SFC of a tempered sample is higher. In this investigation, this shift was observed clearly only for DN, at the tempered temperature. However, until 25 °C, differences were observed between the tempered and untempered samples for all MKFs and beyond 25 °C, they were similar except for DN, which showed a very large difference. This is mainly related to the high amount of StOSt and high amount of POSt present in DN: the higher the amount of StOSt and POSt, the bigger the difference. This indicates that other polymorphic behavior leads to different response to tempering. This result pointed that tempering could be very important in getting the right properties of all MKFs studied. Finally, the various SFC profiles of Ivorian MKFs might be suitable for the design of all purposes type shortening fats.

Polymorphism by XRD

The polymorphism of fat crystals is characterized by the ability of the triacylglycerol (TAG) molecules to arrange themselves in different crystal lattice structures with identical TAG composition [23]. The three basic sub-cell packing

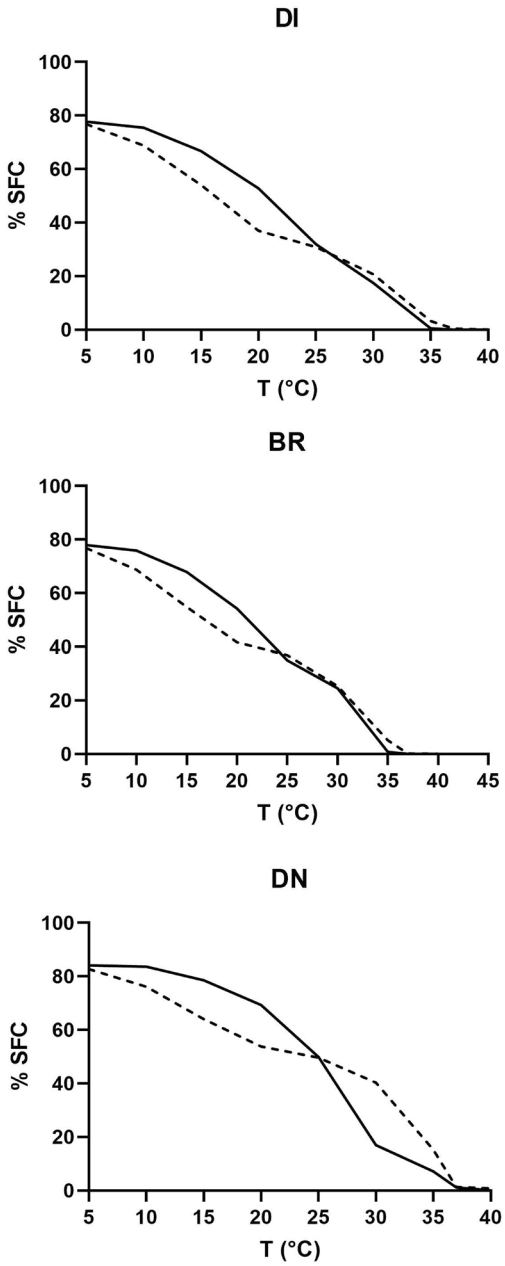

Fig. 3 (continued)

structures of TAG acyl chains are predominant and are known as α, β', and β packing, respectively, of which the thermodynamic stability, the packing density, the melting point, and the melting enthalpy increase in consecutive order [24–26]. The X-ray diffraction patterns in wide-angle scattering (WAXS) of all MKFs obtained during 24 h of static isothermal crystallization at 20 °C are presented in Fig. 4. Except for DN, all samples showed the same type of diffraction pattern of one polymorphic structure, which is β form. All of them showed six main peaks in WAXS with one very strong intensity around 4.60 Å (typical main diffraction peak in WAWS of β structure of fats). Regarding DN, it exhibited diffraction characteristic of more than one crystal structure, with seven main peaks in WAXS at 4.60 Å, 4.37 Å, 4.19 Å, 4.02 Å, 3.87 Å, 3.69 Å, and 3.60 Å. The peak at 3.87 Å and 4.19 Å were typical diffraction patterns of β' structure [27, 28]. The peak at 4.60 Å was a typical main diffraction peak of the β structure. The strongest diffraction intensity implies that, as for the other samples, β was predominant for sample DN solidified under these conditions. The X-ray diffraction patterns of MKF studied here indicated that depending on the variety (different composition), the Ivorian MKF crystallized on the one hand into crystal form β and, on the other hand, in a mixture of crystal structures (β′ and β) throughout 24 h of crystallization at 20 °C. Thus, for all MKF studied, β polymorph appears to be the most prevalent and stable polymorph. By contrast, Sonwai et al. [28] reported a mixture of pseudo-β', β', sub-β, and β polymorphs in all MKF from four different Thai varieties after crystallization at 20 °C for 20 h. Solís-Fuentes et al. [27] examined the evolution of MKF (from Manila variety, Mexico) diffraction patterns from 0 to 26 days of incubation at a temperature of approximately 22 °C and observed that the β form was the predominant and most stable polymorph.

The crystalline structure in Fig. 4, obtained from the analysis of small-angle X-ray scattering (SAXS) patterns of the MKFs studied, shows that although the DN polymorphism is different from other samples, the TAGs present are stacked in similar lamellar configurations (3L or trilayer), except for AM. However, differences in spacings can be observed. Regarding AM, surprisingly, the SAXS pattern showed that both 2L and 3L staking of TAGs are present; a stacking of TAGs with d-spacing of 46.5 Å for 2L and long spacings of 70 Å. According to the literature, 2L structures are formed mostly by long-chain, high-melting, trisaturated TAGs, while 3L structures are usually related to low-melting, long-chain, monounsaturated and mixed long and short-chain TAGs [29, 30]. Thus, the existence of both 3L and 2L packing observed in AM is related to its TAG composition and may particularly suggest a specific interaction like a molecular compound (2L).

Crystal morphology

The polarized light microphotographs (PLM) of the MKFs obtained after static crystallization at 20 °C for 24 h are shown in Fig. 5. Different crystal morphologies were observed among the MKFs. For most of the samples (AM, KI, PR, KT, BR, DI), the microstructure of the fat crystals was disk-shaped, smooth, and had shiny appearance. The Maltese cross could be seen overlaid on the crystals. The crystal size of these fats ranged from 40 to 500 µm. However, for sample AM, PR, KT, and KI, the mean diameter of crystals was higher than those of DI and BR. Some degree

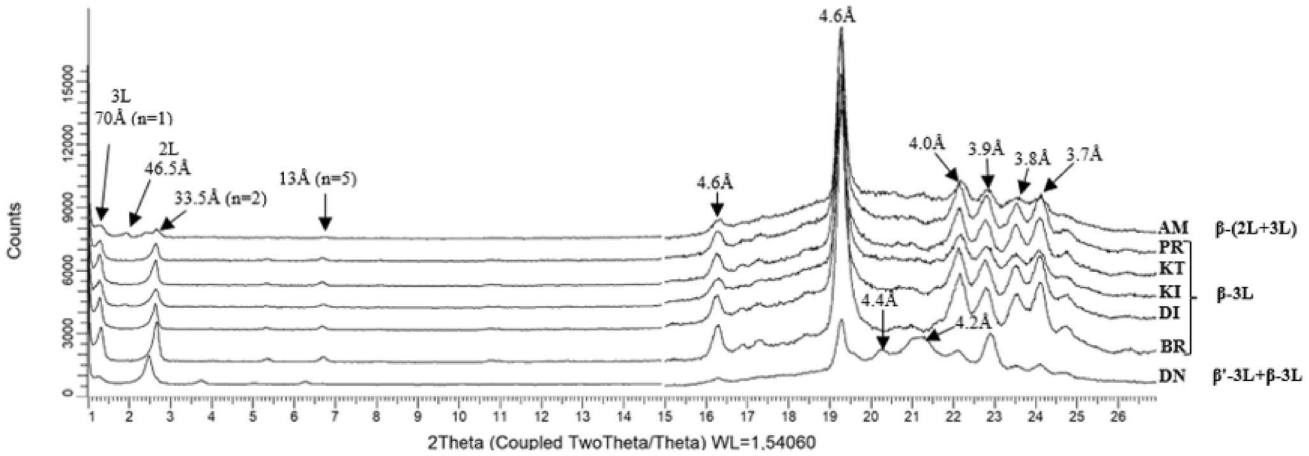

Fig. 4 Small and wide-angle X-ray scattering patterns recorded at the end of static isothermal crystallization at 20 °C for 24 h

of crystal aggregation can be observed for samples BR and DI. In addition, a relatively higher proportion of the liquid phase was observed in the former samples. This can slow down the formation of crystalline nuclei, since the supersaturation, necessary to initiate the crystallization process, is delayed. The microstructure of the DN crystals consisted of both small, disk and spherulites, densely packed, characterizing a mixed morphological type. This simultaneous presence of small disks and spherulites evidence, therefore, a possible polymorphic $\beta' \rightarrow \beta$ transition, confirms the distinct crystallization pattern for this sample. However, the relative higher degree of saturation, on the one hand, and the onset crystallization temperature, on the other hand, of DN may result in the morphological crystal and the compact crystalline structure observed (Fig. 5).

Conclusion

The study of FAC, TAG profile, melting profile, solid fat content, microstructure, and polymorphism of Ivorian MKFs revealed the significant influence of chemical compositions on their general thermal properties. Independently of the variety, the fat of the Ivorian mango kernel is abundant in stearic (St) and oleic (O) fatty acids, with three main TAGs: StOSt (24–45.8%), StOO (15.5–25.8%), and StLSt (10.4–12.5%). All the thermal properties analyzed were linked to the monounsaturated and triunsaturated triacylglycerol content. However, there were significant differences in the chemical composition of MKF from different geographical origins. The seven varieties' studies have been recently grouped according to their main TAG (StOSt) into four groups [10]. The same groups were found in this study by grouping them according to similarities in their physical characteristics. Therefore, the analysis of the results allows to categorize the seven Ivorian varieties into four new subgroups based on both the StOSt wealth and their solid fat content: Hard high-StOSt fat (DN), half-hard medium-StOSt fat (DI, BR), soft low-StOSt fat (KT, PR, KI), and very-soft very-low-StOSt fat (AM). Among the seven samples, the Djakoumankoun (DN) variety, due to its higher SUS content, had the highest melting point and its microstructure was denser at 20 °C. It crystallized under a mixture of β' and β form, whereas under the same conditions, all the other samples studied crystallized only in β form. Therefore, the polymorphism investigation by X-ray diffraction showed that the β-polymorph appears to be the most predominant and stable polymorph for all mango kernel fats under study. On the other hand, Amelie (AM) showed the lowest melting point related to its low SUS and high UUU content. Concluding, the seven Ivorian mango varieties might offer a wide range of applications in the food, pharmaceutical, and cosmetic industries.

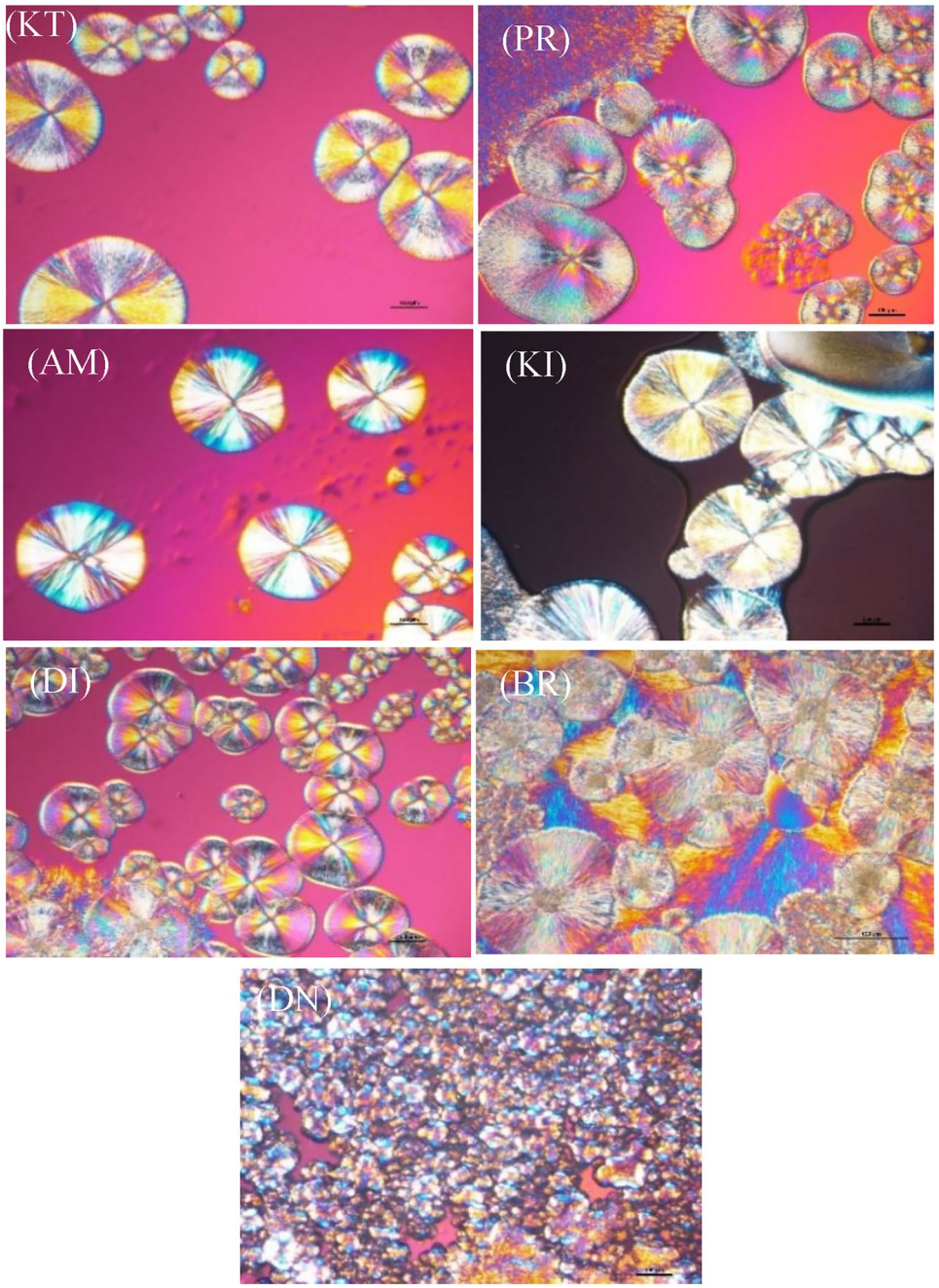

Fig. 5 Polarized light microscope image showing crystal morphology of MKF samples obtained after static crystallization at 20 °C for 24 h

Acknowledgements This research received financial support from the University of Peleforo Gon Coulibaly (Korhogo, Côte d'Ivoire), directed by Prof. Adama Coulibaly, and the University of Liege-Gembloux Agro-Bio Tech (Belgium) (2021/MOB/00080). We would like to thank the Food Science and Formulation Laboratory (University of Liège-Gembloux Agro-Bio Tech, Belgium) for material support. The authors are also grateful to Sandrino Filocco and Lynn Doran for their skilful technical assistance.

Author contributions Alfred Kouakou Kouassi: investigation, conceptualization, formal analysis, methodology, data curation, writing—original draft. Taofic Alabi: supervision, funding acquisition. Elise Amoin N'guessan: investigation, review and editing. Giorgia Purcaro: formal analysis, review and editing. Sabrina Moret: data curation. Mohamed Cissé: investigation. Christophe Blecker: funding acquisition, resources. Sabine Danthine: supervision, methodology, validation, visualization, review and editing.

Data availability The authors confirm that the data supporting the findings of this study are available within the article.

Declarations

Conflict of interest The authors declare no conflict of interest.

Compliance with ethics requirements This study does not involve the participation of human subjects or animals conducted by any of the authors. The research has been conducted in a way that respects the dignity rights and welfare of all the participants.

References

1. FIRCA (2021) Fonds Interprofessionnel pour la Recherche et le Conseil Agricoles. www.firca.ci.
2. Lakshminarayana G, Chandrasekhara Rao T, Ramalingaswamy PA (1983) Varietal variations in content, characteristics and composition of mango seeds and fat. J Am Oil Chem Soc 60(1):88–89. https://doi.org/10.1007/BF02540898
3. Nzikou JM, Kimbonguila A, Matos L, Loumouamou B, Pambou-Tobi NPG, Ndangui CB, Abena AA, Silou T, Scher J, Desobry S (2010) Extraction and characteristics of seed kernel oil from mango (*Mangifera indica*). Res J Environ Earth Sci 2(1):31–35
4. Solís-Fuentes JA, del Carmen Durán-de-Bazúa M (2020) Mango Seed: Mango (*Mangifera indica* L.) seed and its fats. In: Nuts and Seeds in Health and Disease Prevention (pp. 79–90). Academic Press. https://doi.org/10.1016/B978-0-12-375688-6.10088
5. Official Journal of the European Communities (2000) Directive of 23 June 2000 relating to cocoa and chocolate products intended for human consumption. Directive 2000/36/EC, 19, L197
6. Kaur G, Kaur D, Kansal SK, Garg M, Krishania M (2022) Potential cocoa butter substitute derived from mango seed kernel. Food Chem 372:131244. https://doi.org/10.1016/j.foodchem.2021.131244
7. Solís-Fuentes, J. A., & DurándeBazúa, M. C, (2004) Mango seed uses: thermal behavior of mango seed almond fat and its mixtures with cocoa butter. Bioresour Technol 92(1):71
8. Sonwai S, Kaphueakngam P, Flood A (2014) Blending of mango kernel fat and palm oil mid-fraction to obtain cocoa butter equivalent. J Food Sci Technol 51(10):2357–2369. https://doi.org/10.1007/s13197-012-0808-7
9. Jin J, Warda P, Mu H, Zhang Y, Jie L, Mao J, Xie D, Huang J, Jin Q, Wang X (2016) Characteristics of mango kernel fats extracted from 11 China-specific varieties and their typically fractionated fractions. J Am Oil Chem Soc 93(8):1115–1125. https://doi.org/10.1007/s11746-016-2853-2
10. Kouassi AK, Alabi T, Cissé M, Purcaro G, Moret S, Moret E, Moret E, Blecker C, Danthine S (2023) Assessment of composition, color, and oxidative stability of mango (*Mangifera indica* L.) kernel fats from various Ivorian varieties. J Am Oil Chem Soc. https://doi.org/10.1002/aocs.12758
11. Kouassi AK, Alabi T, Purcaro G, Moret E, Blecker C, Danthine S (2023) Thermal and structural behavior of mango (*Mangifera indica* L.) kernel fat from three Ivorian varieties. J Am Oil Chem Soc. https://doi.org/10.1002/aocs.12781
12. Mtibaa I, Zouari A, Purcaro G, Attia H, Ayadi MA, Danthine S (2021) Crystallization mechanisms in camel milk cream during physical ripening: effect of temperature and ripening duration. Food Bioprod Process 127:435–442. https://doi.org/10.1016/j.fbp.2021.03.016
13. IUPAC (1987) Solid Content Determination in Fats by NMR (low-resolution nuclear magnetic resonance) Norm Version 1987: 2.150 (ex 2.323) (1987)
14. Danthine S (2012) Physicochemical and structural properties of compound dairy fat blends. Food Res Int 48(1):187–195
15. AOCS Methods (2009) Official methods and recommended practices of the AOCS. 6th ed. Urbana, III: AOCS 2009
16. Jin J, Jin Q, Akoh CC, Wang X (2021) StOSt-rich fats in the manufacture of heat-stable chocolates and their potential impacts on fat bloom behaviors. Trends Food Sci Technol 118:418–430. https://doi.org/10.1016/j.tifs.2021.10.005
17. Lieb VM, Schuster LK, Kronmüller A, Schmarr HG, Carle R, Steingass CB (2019) Fatty acids, triacylglycerols, and thermal behavior of various mango (*Mangifera indica* L.) kernel fats. Food Res Int 116:527–537. https://doi.org/10.1016/j.foodres.2018.08.070
18. Jahurul MHA, Zaidul ISM, Norulaini NN, Sahena F, Abedin MZ, Ghafoor K, Omar AM (2014) Characterization of crystallization and melting profiles of blends of mango seed fat and palm oil mid-fraction as cocoa butter replacers using differential scanning calorimetry and pulse nuclear magnetic resonance. Food Res Int 55:103–109. https://doi.org/10.1016/j.foodres.2013.10.050
19. Braipson-Danthine S, Deroanne C (2006) Determination of solid fat content (SFC) of binary fat blends and use of these data to predict SFC of selected ternary fat blends containing low-erucic rapeseed oil. J Am Oil Chem Soc 83(7):571–581. https://doi.org/10.1007/s11746-006-1242-7
20. Talbot G (2009) In: Beckett ST (ed) Industrial chocolate manufacture and use. *Wiley-Blackwell*, Oxford, chap 19, pp 415–433. https://doi.org/10.1002/9781444301588
21. Timms RE (2003) Confectionery fats handbook: properties, production and application. Oily Press, Bridgwater, p 441
22. Beckett ST (ed) (2011) Industrial chocolate manufacture and use. Wiley, Hoboken. https://doi.org/10.1002/9781444301588
23. Declerck A, Nelis V, Danthine S, Dewettinck K, Van der Meeren P (2021) Characterisation of fat crystal polymorphism in cocoa butter by time-domain NMR and DSC deconvolution. Foods 10(3):520. https://doi.org/10.3390/foods10030520
24. Sato K (2001) Crystallisation behavior of fats and lipids—a review. Chem Eng Sci 56(7):2255–2265. https://doi.org/10.1016/S0009-2509(00)00458-9
25. Ribeiro APB, Basso RC, Gonçalves LAG, Gioielli LA, Dos Santos AO, Cardoso LP, Kieckbusch TG (2012) Physicochemical properties of Brazilian cocoa butter and industrial blends. Part II Microstructure, polymorphic behavior and crystallisation characteristics. Grasas Aceites 63(1):89–99. https://doi.org/10.3989/gya.069111
26. Marangoni AG (2018) Structure-function analysis of edible fats, 2nd edn. Elsevier, Amsterdam. https://doi.org/10.1016/C2017-0-00579-7
27. Solís-Fuentes JA, del Rosario Hernández-Medel M, del Carmen Durán-de-Bazúa M (2005) Determination of the predominant polymorphic form of mango (*Mangifera indica*) almond fat by differential scanning calorimetry and X-ray diffraction. Eur J Lipid Sci Technol 107(6):395–401. https://doi.org/10.1002/ejlt.200401072
28. Sonwai S, Ponprachanuvut P (2014) Studies of fatty acid composition, physicochemical and thermal properties, and crystallisation behavior of mango kernel fats from various Thai varieties. J Oleo Sci 63(7):661–669. https://doi.org/10.5650/jos.ess14036
29. Hagemann, J. W (1988) Thermal behavior and polymorphism of acylglycerides. Kapitel 2 In: Garti N. and Sato K. (Ed.) Crystallisation and polymorphism of fats and fatty acids

30. A. Karleskind and J. P. Wolff (1992) Manuel des corps gras. AFECG, Ed., Lavoisier, Paris, chap. 5